Iver E. Anderson
Metal & Ceramic Sciences Program, Ames Laboratory (USDOE),
Iowa State University, Ames, IA. 50011, USA
E-mail: andersoni@ameslab.gov; Telephone: (515) 294-9791; FAX: (515) 294-8727

Brian Gleeson
Metal & Ceramic Sciences Program, Ames Laboratory (USDOE),
Iowa State University, Ames, IA. 50011, USA
E-mail: gleeson@ameslab.gov; Telephone: (515) 294-4446; FAX: (515) 294-8727

Robert L. Terpstra
Metal & Ceramic Sciences Program, Ames Laboratory (USDOE),
Iowa State University, Ames, IA. 50011, USA
E-mail: terpstra@ameslab.gov; Telephone: (515) 294-5747; FAX: (515) 294-8727

# Development of Metallic Filters for Hot Gas Cleanup in Pressurized Fluidized Bed Combustion Applications

Keywords: metal filters, PFBC, Ni-base superalloys, metal powder processing

## Introduction

The pressurized fluidized bed combustion (PFBC) process has been developed to be a highly efficient, high-temperature combustion technique to burn coal containing high levels of sulfur. Unfortunately, a major barrier to the implementation of the PFBC process has been the design of a robust hot gas filter material that possesses adequate corrosion resistance (Terpstra et al. 2001) The filter must remove abrasive/corrosive "flyash" particulate from the hot, typically about 850°C, oxidizing/sulfidizing combustion gas to protect the gas turbine generator located downstream of the PFBC combustion zone. Initially, an array of multiple ceramic cylindrical "candle" filters was adopted to provide a copious amount of filtration area. However, the current ceramic filters appear to be too brittle to withstand typical operating conditions and procedures (Oakey et al. 1997, Oakey et al. 1995, Alvin 1995). As a result, porous metal filters are being developed and considered as alternative devices to advance the PFBC process.

Generally, metallic materials used in PFBC applications will need to rely on the formation and preservation of a slow-growing $Al_2O_3$ scale to protect the base metal from the surrounding environment. Formation of such an oxide scale is controlled by the diffusion kinetics between the aluminum constituent of the base alloy and the oxygen-bearing component in the combustion gas. To protect the base material, the oxide scale must react slowly with the surrounding environment and must form a continuous and adherent metallic oxide layer capable of enduring the effects of both growth and thermal stresses (Gleeson 2000) As the thickness of the oxide layer increases, it becomes significantly less strain tolerant and prone to spallation due, for example, to growth defects and thermal stresses. Healing or reformation of the alumina scale can occur in the event of scale cracking or spallation if a sufficient amount of aluminum is available for oxidation at the alloy surface. However, the finite thickness of the

alloy component places a practical limit on the reservoir of aluminum and, hence, on the duration of sustained alumina-scale growth. Eventually, the aluminum content in the alloy will be depleted below a level necessary for chemical equilibrium between the alloy and the alumina scale. At this point, "chemical" breakdown of the alumina scale results and formation of less protective oxides of the base metal ensues (Quadakkers 1994).

Metallic filters based on the $Fe_3Al$ (iron aluminide) intermetallic compound have been well developed as an alternate material for the ceramic hot gas filters. Compared with SiC and $Al_2O_3$ filter materials, the iron aluminide filters offer a slight improvement in strength and resistance to thermal shock at the anticipated PFBC operating temperature of 850°C. Unfortunately, the brittle properties of the iron aluminides at ambient temperature are similar to ceramics and their strength at 850°C is not sufficient to resist creep elongation. Iron aluminides have also proven very difficult to weld, an important alloy property for the successful fabrication of full-scale candle filter systems. In addition, the powder processing route that was selected for commercial application of iron aluminides resulted in thick-walled filters that have a considerable weight penalty, compared to ceramic candle filters of the same filter area.

**Objective**

Alternative alloys derived from the wide array of aerospace superalloys will be developed for hot gas filtration to improve on both ceramic filters and "first-generation" iron aluminide metallic filter materials. New high performance metallic filters should offer the benefits of non-brittle mechanical behavior at all temperatures, including ambient temperature, and improved resistance to thermal fatigue compared to ceramic filter elements, thus improving filter reliability. A new powder processing approach also will be established that results in lightweight metallic filters with high permeability and weldability for enhanced capability for filter system manufacturing.

**Approach**

The first set of candidate alloys will be limited to those which form an alumina ($Al_2O_3$) scale under oxidizing/sulfidizing conditions found in PFBC systems at temperatures up to about 850°C. An example of an alumina-forming commercial cast and wrought alloy which has been shown to be protective under such conditions is "Haynes 214" (nominal composition in wt.%): 75Ni-16Cr-4.5Al-3Fe-0.05C-0.01Y-0.05Mn-0.2Si-0.1Zr-0.01B, denoted as Ni-Cr-Al-Fe in this paper. An advantage of selecting commercial alloys is that their weldability has been determined and appropriate weld filler materials have been designated. Further, they have been alloyed for scale spallation resistance during thermal cycling and for high-temperature creep strength.

A high pressure gas atomization (HPGA) process, developed at Ames Laboratory, will be utilized to produce sufficient quantities of powder for this initial stage of porous filter material testing from selected alloy compositions. One characteristic of the HPGA process that is shared by most commercial manufacturers of aerospace grade superalloy (Ni and Co based) powders is both an inert atmosphere melting chamber and atomization spray chamber, preferably vacuum pumped prior to backfilling. These atomization system features can promote a very low pick-up of interstitial impurities in the melt and an extremely low level of oxide (or nitride) surface film formation on atomized powder particles.

Using the benefits of these "clean" superalloy powders, a unique spherical powder processing and solid state sintering approach will be developed to fabricate metallic filters having uniform, closely controlled

porosity. Moreover, the advanced powder processing and sintering techniques will permit additional filter design capability for highly controlled filter porosity/permeability, enabling more efficient filtration, and will provide greatly simplified filter system manufacturing.

The corrosion resistance of the filter materials will be evaluated under simulated PFBC/IGCC gaseous environments in order to determine the optimum alloy composition and filter structure, using a commercial iron aluminide alloy as a baseline. The corrosion tests will also provide a means to estimate the service lives of experimental filter materials when subjected to either normal or abnormal PFBC/IGCC plant operating conditions.

**Project Description**

The Ni-Cr-Al-Fe filter material developed at Ames Laboratory appears to offer significant benefits over both the ceramic and iron aluminide materials (Terpstra et al. 2001). The Ni-Cr-Al-Fe alloy has shown the ability to maintain a nearly equivalent resistance to corrosion as the iron aluminide in initial sulfidizing/oxidizing corrosion tests at 850°C for up to 1,000 hours. Also, the 850°C yield strength of the porous sintered Ni-Cr-Al-Fe material was observed to be at least 6 times that of the iron aluminides, while maintaining excellent room temperature ductility (Terpstra et al. 2001).

Based on the results of our initial studies, the premise of this study was that the service life of a metallic hot gas filter could be extended if sufficient aluminum were available for oxidation. Thus, this study investigated the influence of increasing the aluminum content of the Ni-Cr-Al-Fe alloy that was previously studied. Corrosion resistance to simulated PFBC operating conditions for 1,000 hours and yield strength over a range of temperatures were observed as the aluminum content was increased up to three times the base Ni-Cr-Al-Fe alloy. This study also investigated the potential of resistance spot welding and forming thin (0.5 mm) porous sintered sheets into welded cylindrical shapes for further testing.

**Results**

Corrosion Tests

A high-temperature corrosion testing system was used to assess the long-term scaling resistance of the chill-cast candidate alloys containing 2 and 3 times more aluminum content than the initial Ni-Cr-Al-Fe alloy of our study. In the modified alloys, the Al content was elevated at the expense of the same wt.% amount of Ni, using commercial ingot of Haynes 214 as a masteralloy. The base and modified alloys were tested as chill-castings in both the "as-received" and a "pre-oxidized" conditions. Pre-oxidation consisted of exposing the alloy sample to flowing argon gas for 50 hrs. at 1,000° C. The purpose of the pre-oxidation treatment was to facilitate the formation of slow growing alumina as a continuous scale, preferably between 1 – 4 μm, thick to protect the base metal before being exposed to the oxidizing/sulfidizing test environment. To reproduce the typical PFBC oxidizing/sulfidizing combustion environment, samples were exposed to a flowing $N_2$ – 13 $CO_2$ – 10 $H_2O$ – 4 $O_2$ – 250 ppm $SO_2$ (in vol.%) gas mixture at 850° C for 1,000 hours. The samples were cooled to room temperature every 250 hours to record their weight change.

As a review of previous relevant data (Terpstra et al. 2001), Figure 1 shows a comparison in the weight-change behavior of the reference Ni-Cr-Al-Fe alloy, a $Fe_3Al$ alloy, and one of the current modified

alloys in the as-received and pre-oxidized ("pre-ox") conditions. As shown, the weight change of the as-received Ni-Cr-2xAl-Fe alloy, having twice the aluminum content as the reference Ni-Cr-Al-Fe alloy, is approximately half that of the as-received base alloy. The influence of the pre-oxidation treatment relative to the as-received sample condition is also shown in Figure 1. As can be seen, the pre-oxidized samples underwent significantly less weight gain than all of the as-received samples for the entire test period.

The weight-change kinetics of the pre-oxidized samples is more clearly shown in Figure 2. As can be seen in this figure, the weight change for the pre-oxidized alloys is very small and there is little difference in the corrosion resistance under the conditions tested. As suggested earlier, if the aluminum within the alloy is the sole source for sustaining alumina-scale growth, then the more aluminum that is available in the alloy, the longer the filter material should survive by prolonging chemical breakdown of the alumina scale. Based on this premise and the demonstrated beneficial influence of the "pre-oxidation" treatment, the possibility of increasing the corrosion resistance of an alloy should be achieved with an alloy that has a high aluminum content and is pre-oxidized. It should be noted, however, that weldability and toughness constraints place a practical limit on the amount of aluminum that can be added to the alloy. That limit was found to be approximately three times the amount in the Ni-Cr-Al-Fe base metal. Accordingly, results will be presented for only the 2xAl and 3xAl alloys, together with the base alloy.

Figure 3 shows the weight-gain kinetics for the modified alloys tested in the as-received and pre-oxidized states. The best performing alloy is seen to be pre-oxidized 2xAl. Interestingly, the 2xAl alloy performed better than the 3xAl alloy, either with or without pre-oxidation. This may be associated with the 3xAl alloy being overly brittle and consequently resulting in a greater frequency of scale cracking events, particularly during cooling after every 250 h of testing.

The superior corrosion performance of the pre-oxidized 2xAl alloy ingot prompted the atomization of the 2xAl alloy into powder. To simulate a metal filter element, gas atomized powder of the Ni-Cr-2xAl-Fe alloy, sized 25 μm < dia. < 45μm, was sintered to approximately a 70% density and exposed to the environmental test condition previously described. Figure 4 shows the weight-change results for both the as-received and the pre-oxidized cast and porous compacted samples. As can be seen, the weight change experienced by the porous sample was significantly higher than the ingot sample, primarily due to the increased surface area of the porous sample exposed to the corrosive gas (*i.e.*, only the gross dimensional surface area was considered for the porous sample). However, the pre-oxidizing treatment remained extremely beneficial for limiting the weight change of the porous sintered 2xAl sample, relative to the as-received porous sample.

Protecting the base metal from the corrosive gas environment can be accomplished or at least minimized by forming a continuous alumina scale between the base metal and the corrosive gas. With continued alumina growth, the subsurface of the alloy becomes depleted in aluminum, eventually to the extent that internal oxidation of the aluminum and void formation may result. Such subsurface degradation is the precursor to breakdown of the protective alumina scale. Figure 5 shows cross-sectional SEM micrographs of various pre-oxidized samples after 1,000 h testing. The 2xAl alloy is seen to form a thin, continuous scale layer with no clear evidence of subsurface degradation. The 3xAl alloy also developed a protective scale; however, rectangular internal precipitates in the vicinity of the alloy/scale interface were evident. It is inferred from the rectangular morphology of these precipitates that they are

aluminum nitride, AlN (Lai 1990). Apparently, increasing the aluminum content in the alloy increases the preferential reactivity of aluminum to nitridation. The SEM image of the sintered powder, shown in Fig. 5c, reveals that a continuous protective oxide layer develops on powders of sufficient size and that the oxide layer does not jeopardize the inter-particle bond developed during the sintering cycle. However, powders less than about 15 μm in diameter had a limited reservoir for sustaining alumina scale growth throughout the 1,000 h test, as indicated by the fact that such powders underwent extensive attack (*i.e.*, some were through-corroded).

Yield Strength Results:

Figure 6 illustrates the yield strength, using an asymmetric four point bend (AFPB) test procedure and a strain rate of 0.1 mm/min., of several currently used and potential hot gas filter materials tested in air over a range of typical operating temperatures. As shown in the figure, the porous ceramic materials, $Al_2O_3$ and SiC, demonstrated a very low, yet consistent yield strength for all the temperatures tested. A yield strength rise can be noted at 600° C for the Ni-Cr-3xAl-Fe chill-cast sample, perhaps due to a pronounced precipitation hardening effect promoted at the test temperature. Comparing the bulk samples, the Ni-Cr-2xAl-Fe alloy exhibited the highest yield strength at both room temperature and at 850° C. At this temperature, all of the alloys, including the porous Ni-Cr-Al-Fe sample, demonstrated equal or higher yield strengths than the $Fe_3Al$ alloy. Also notable is that in bulk form at 850°C, the yield strength of the Ni-Cr-2xAl-Fe is nearly twice that observed for the Ni-Cr-Al-Fe alloy.

Sintering Tests:

The corrosion results and the yield strength data verified the selection of the Ni-Cr-2xAl-Fe alloy for extensive development and testing of porous filter sheet material. Preliminary indications of brittleness for porous sheets of this alloy were eliminated by employing an extended sintering cycle to promote an enhanced state of bonding between sintered particles, as shown by comparing the SEM micrographs in Figure 7a and 7b. The extended sintering cycle maintained the simplicity of the sheet bonding process, without the need for post-sintering heat treatment. With this sintering method and an alumina mold, having a cavity of 3.8 mm x 25.4 mm x 0.5 mm, large porous sheet samples could be successfully produced without the aid of a mold release coating, where slight sintering shrinkage permitted mold release. The resulting 0.5 mm thick porous sintered sheet samples were rolled to a diameter equal to the outside diameter of a typical candle filter, indicating that the ambient temperature ductility of the porous material was sufficient for this application.

Resistance Spot Welding:

Resistance spot welding trials were conducted on the 0.5 mm thick strips of porous sintered Ni-Cr-2xAl-Fe material using a 20kVA resistance seam welder, Black & Webster model SWHD 850, adapted to a resistance spot weld mode. There are several factors that influence a spot weld process. Figure 8 shows cross-sectional micrographs of resistance spot welds formed in this study using weld power levels of 10 and 15 kVA while maintaining a consistent total weld time of 66 ms. As shown, the welds formed using these 2 power setting resulted in weld zones having different microstructures. The weld re-solidification zone produced using the 10kVA setting appears to have developed a fine equiaxed grain size with some apparent microvoids at the grain triple points. In contrast, more extensive fusion is evident in the 15 kVA weld of Figure 8b, where a partially dendritic re-solidification pattern developed It is significant to

note that both power levels produced welds that bonded the porous sheets from the interior contact surfaces, with exterior porosity remaining intact. This weld joint characteristic appears to have helped prevent cracking by distributing post weld stresses.

**Application**

Corrosion resistance of a type of Ni-Cr-Al-Fe alloy in bulk form has been improved to become comparable to the corrosion resistance of a commercially available $Fe_3Al$ alloy for use in a PFBC system through selective alloy design. Based on resistance to an oxidation/sulfidation gas atmosphere and yield strength observations in bulk samples, doubling the aluminum content was found to be more beneficial than further increases in the aluminum content of the base alloy. Further improvements in the corrosion resistance of the Ni-Cr2xAl-Fe alloy, however; may be needed to enhance the service life of porous hot gas filters made from alloy powders. With respect to the processes for fabrication of metallic hot gas filters, doubling the alloy aluminum content did not impair sintering of the tap-densified powders, while the resulting thin porous sheet retained sufficient ductility for roll forming. The Ni-Cr-2xAl-Fe alloy also demonstrated the ability to be joined using conventional resistance spot welding techniques. Figure 9 illustrates a 60.3 mm diameter rolled and welded "o-ring " prototype filter sample, having a 0.5 mm wall. The prototype filter was fabricated using 25 < dia. <45 μm Ni-Cr-2xAl-Fe powder that was vacuum sintered to approximately a 70% density and joined using a series of resistance spot welds at 10 kVA for 66 ms.

**Future Activities**

Having the ability to roll and weld the o-ring filter shape now allows porous sintered samples to be placed in a DOE-supported combustion facility, e.g., EERC at Grand Forks, ND, or in a commercial PFBC/IGCC system for long term corrosion testing and evaluation of fly ash deposition effects. Eventually, a joining process for end caps and termination flanges will need to be developed to produce thin-walled metallic filter elements for in-situ prototype testing planned for at a later stage of this project.

While long term combustion atmosphere tests are in progress, a new round of corrosion testing will be initiated to select a limited set of alloy candidates that can tolerate IGCC environments. Initial screening experiments will be conducted with as-fabricated bulk specimens at 650˚C for up to 1000 h in a 150 $cm^3$/min flowing gas mixture at a total pressure of 1 atm. Two gas-mixture compositions will be studied in order to simulate basic oxidizing and reducing environments that a hot gas filter may encounter in IGCC service. The approximate compositions of the gas mixtures will be as follows:

Oxidizing: $N_2$ – 13 $CO_2$ – 10 $H_2O$ – 4 $O_2$ – 250 ppm $SO_2$

Reducing: $N_2$ – 24 CO – 5 $CO_2$ – 5 $H_2O$ – 14 $H_2$ – 1.3 $CH_4$ – 20 ppm $H_2S$

The corrosion behavior and kinetics of the various alloys will be determined from weight-change measurements and microstructural examination of metallographically-prepared cross-sections of the corroded specimens. Cross-sectional analyses will allow for determination of the rate of metal wastage. The targeted allowable wastage rate will be about 1.5 μm/year. The results from these tests will select a

limited set of alloy candidates for IGCC applications to conduct further testing in a pre-oxidized condition and to initiate powder processing experiments, leading to filter sample characterization. In addition to inclusion of some of the promising alloys from the PFBC studies in the IGCC tests, a second set of IGCC candidate alloys will be tested which form a thin duplex scale of $SiO_2$ and $Cr_2O_3$ (such scales are typically thinner than single-layered $Cr_2O_3$ scales). There is experimental evidence which indicates that such alloys are resistant to oxidizing/sulfidizing conditions containing trace chlorine (Bakker 1995). The following commercial alloys are listed as examples (nominal compositions in wt.%):

Haynes HR-160 alloy: 37Ni-29Co-28Cr-2Fe-2.75Si-0.05C

Inco alloy 330: 35.5Ni-18.5Cr-44Fe-1.2Si-2Mn

Krupp alloy 45TM: 47Ni-27Cr-23Fe-2.7Si-0.08C 0.01Y

Similar to the alumina-forming commercial alloys, these alloys are weldable, with the weld filler materials having already been determined. In addition, they have been alloyed for scale spallation resistance during thermal cycling and for high-temperature creep strength. Support from DOE-Fossil Energy, Advanced Research and Technology Development (ARTD) Program through Ames Lab contract no. W-7405-Eng-82 is gratefully acknowledged.

**References**


1. Terpstra, R. L., Anderson, I. E., B. Gleeson (2001), “Development of Metallic Hot Gas Filters," in Advances in Powder Metallurgy and Particulate Materials, MPIF-APMI, Princeton, NJ, Vol. 8, (2001) p.84.

2. Oakey, J.E., Lowe. T., Morrel, R., Byrne, W. P., Brown, R., and Stringer J., Materials at High Temperatures, 14, (1997) p. 301.

3. Oakey, J.E., Lowe, T., Morrel, R., Stringer, J., and Brown, R., in Proc. 2nd International Conference on Heat-Resistance Materials, K. Natesan et al. (eds.), ASM International, Materials Park, OH, (1995) p. 537.

4. Alvin, M. A., in Proc. 2nd International Conference on Heat-Resistant Materials, K. Natesan et al. (eds.), ASM International, Materials Park, OH, (1995) p. 525.

5. Gleeson, B., "High-Temperature Corrosion of Metallic Alloys and Coatings," in Corrosion and Environmental Degradation, Vol. II: Volume 19 of the Materials Science and Technology Series, ed. M. Schutze (Weinheim, Germany: Wiley-VCH), (2000) p. 173.

6. Quadakkers, W.J., Bennett M.J., *Mater. Sci., Technol*., 10, (1994) p. 126.

7. Lai, G.Y., *High-Temperature Corrosion of Engineering Alloys*, ASM International, Materials Park, OH, (1990) p.82.

8. Bakker, W. T. (1995) *Mixed Oxidant Corrosion in Nonequilibrium Syngas at 540° C*, EPRI TR-104228.

**Figures and Tables**

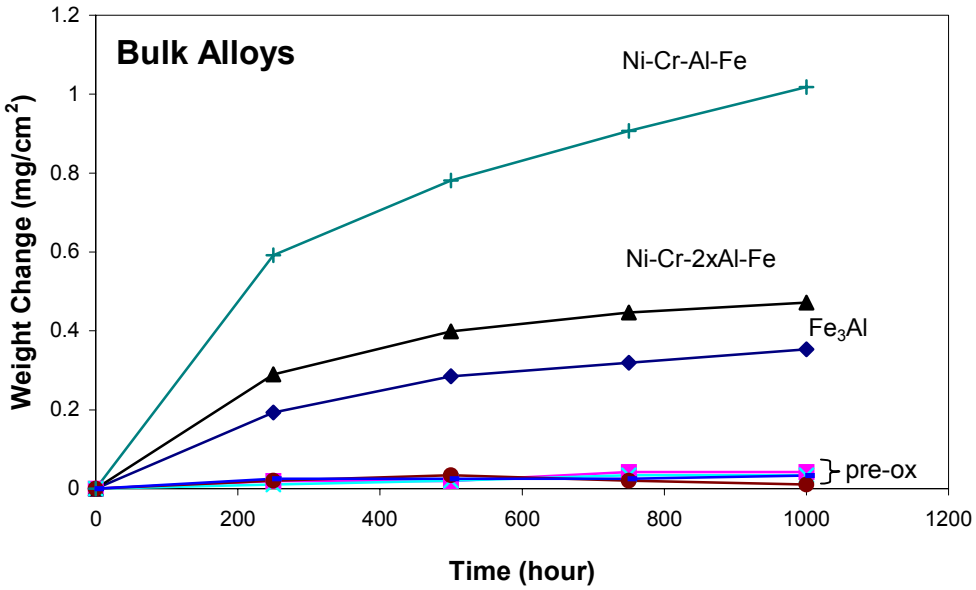


Figure 1. Corrosion test results of pre-oxidized and as-received bulk alloys exposed to $N_2$-13$CO_2$-10$H_2O$-4$O_2$-250 ppm $SO_2$ (vol. %) gas for 1,000 h at 850° C.

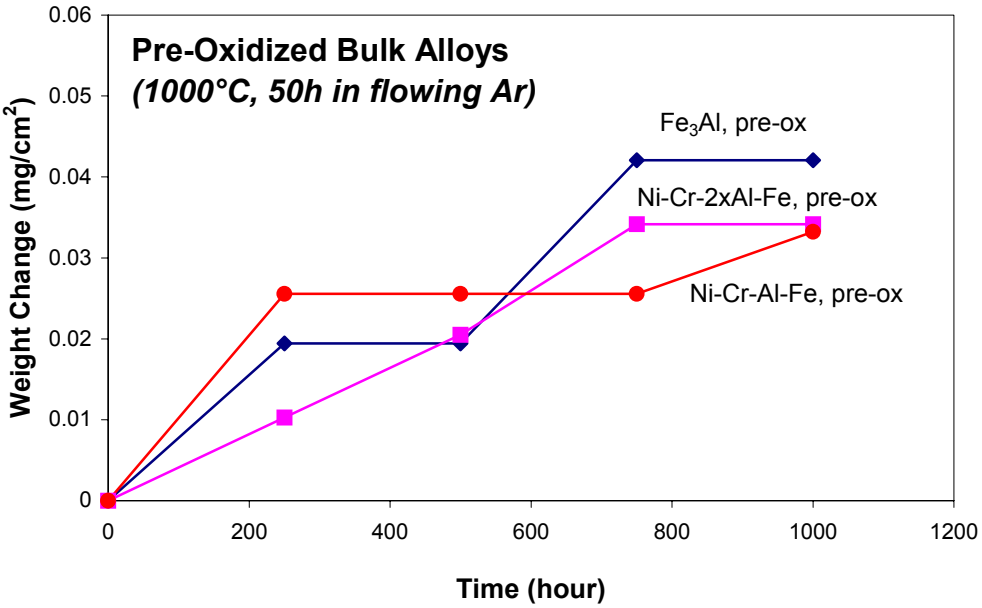


Figure 2. Corrosion test results of pre-oxidized bulk alloys exposed to $N_2$-13$CO_2$-10$H_2O$-4$O_2$-250 ppm $SO_2$ (vol. %) gas for 1,000 hrs. at 850°C.

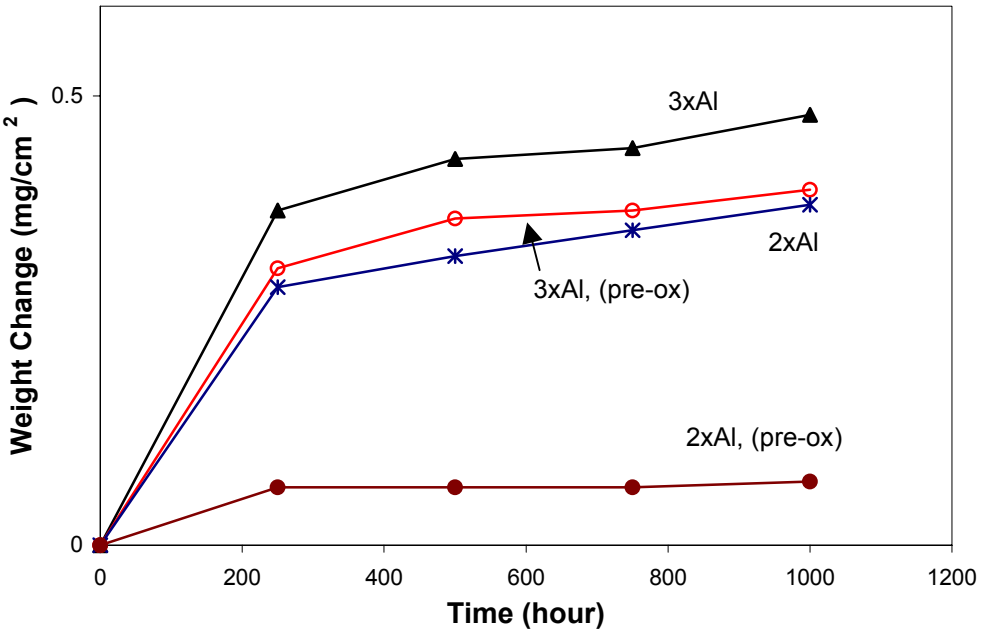


Figure 3. Corrosion test results of aluminum-enriched Ni-Cr-Al-Fe alloy ingots exposed to $N_2$-13$CO_2$-10$H_2O$-4$O_2$-250 ppm $SO_2$ (vol. %) gas for 1,000 hrs. at 850° C.

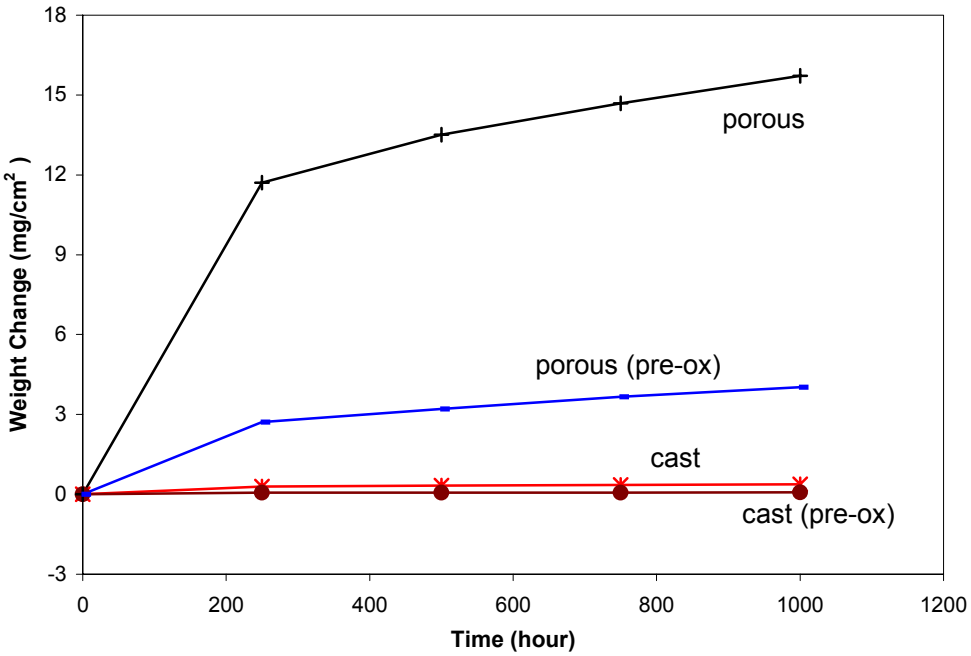


Figure 4. Corrosion test results of Ni-Cr-2xAl-Fe, showing as-cast and sintered porous samples exposed to $N_2$-13$CO_2$-10$H_2O$-4$O_2$-250 ppm $SO_2$ (vol. %) gas for 1,000 hrs. at 850° C.

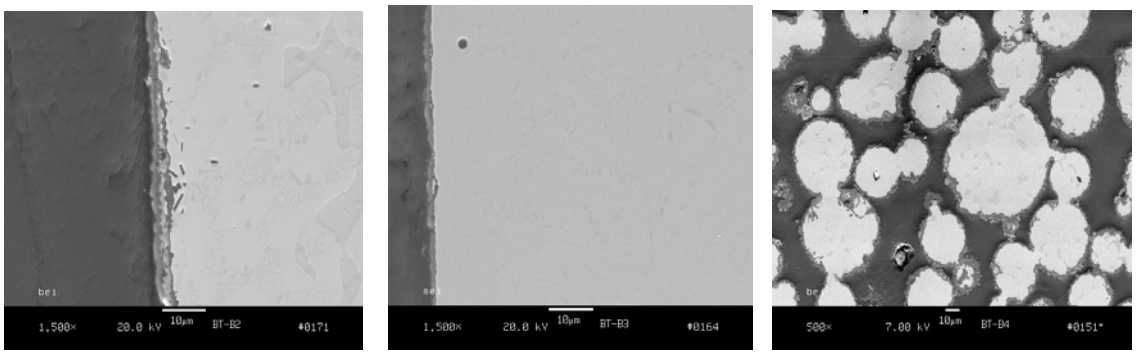

a) Ni-Cr-3xAl-Fe b) Ni-Cr-2xAl-Fe, c) Ni-Cr-2xAl-Fe Sintered Powder

Figure 5. Cross sectional SEM images of pre-oxidized samples.

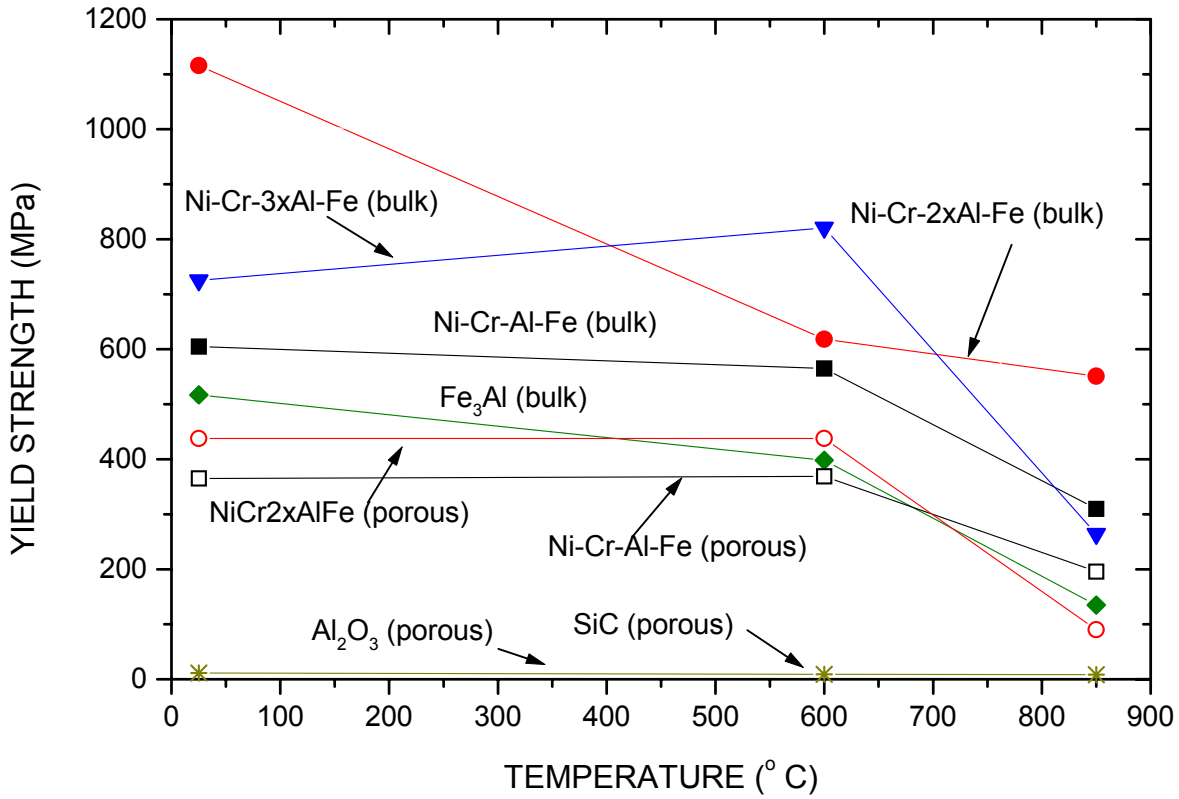


Figure 6. Yield strength results from asymmetric four point bend (AFPB) tests, performed at the indicated temperatures.

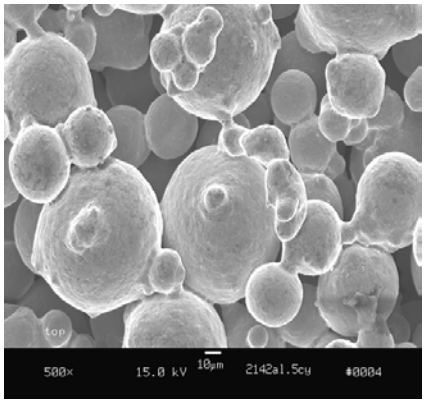


a) 0.5 hr. @ 1250° C

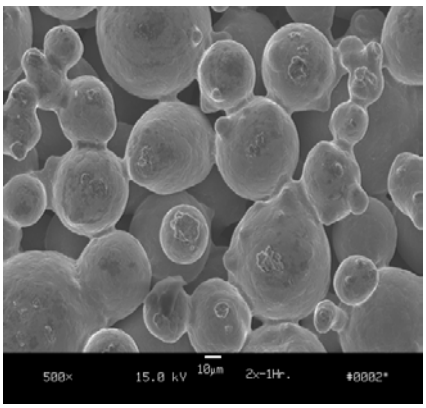


b) 1.0 hr. @ 1250° C

Figure 7. SEM images of sintered Ni-Cr-2xAl-Fe powder, 25 µm > dia. < 45 µm.

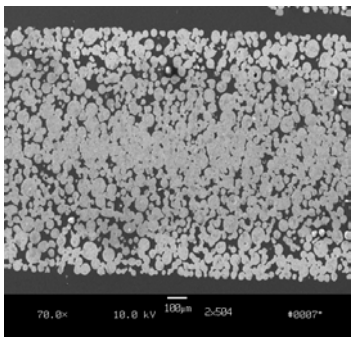


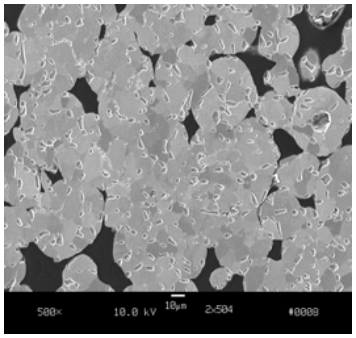


a)

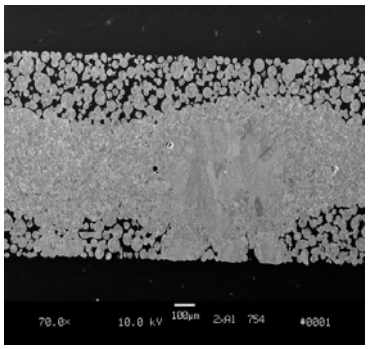


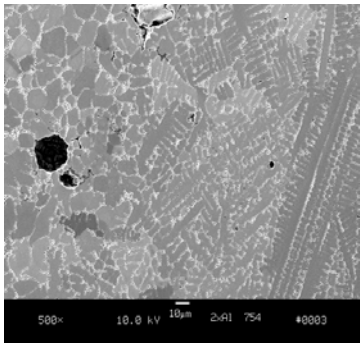


b)

Figure 8. SEM images of Ni-Cr-2xAl-Fe resistance spot welds using a) 10 kVA, and b) 15 kVA.

Figure 9. Resistance spot welded porous cylinder of sintered Ni-Cr-2xAl-Fe powder.